Fine tuning and measurement of mechanical properties of crosslinked hyaluronic acid hydrogels as biomimetic scaffold coating in regenerative medicine

*Caterina Credi**, *Serena Biella*, *Carmela De Marco*, *Marinella Levi*, *Raffaella Suriano*, *Stefano Turri*

Department of Chemistry, Materials and Chemical Engineering "Giulio Natta", Politecnico di Milano, Piazza Leonardo da Vinci 32, 20133 Milano, Italy

Received 27 July 2013 Received in revised form
17 September 2013
Accepted 21 September 2013 Available online 4
October 2013

1. Introduction

Adult stem cells (SCs) are specialized and essential for tissue maintenance and repair (Hachet et al., 2012; Discher et al., 2005). In the body, SCs reside within instructive tissue specific niches which regulate SCs fate providing proper chemical and mechanical stimuli. Consequently, mimicking such tridimensional environment in vitro is the main goal of regenerative medicine and is challenging to understand the role of each specific aspect in affecting SCs differentiation. Actually, the most promising strategy involves seeding SCs on a scaffold, an interim synthetic extracellular matrix, culturing them giving proper cues until maturation into a functional tissue ready to be transplanted in an injured patient (Kim et al., 2011). Recent studies highlighted the fundamental effect that mechanical properties of the artificial in vitro environment have on many aspects of cell functions including adhesion, migration, proliferation (Hachet et al., 2012) and on differentiation (Discher et al., 2005; Evans et al., 2009). In particular, after several weeks in culture, mesenchymal stem cells (MSCs) are

**Corresponding author*. Tel.: +39 22 399 3213.
E-mail address: caterina.credi@chem.polimi.it (C. Credi).

proved to commit to the lineage specified by matrix elasticity and substrate stiffness they sense: soft matrices (0.1÷1 kPa) are neurogenic, stiffer matrices (8÷17 kPa) are myogenic and rigid matrices (10÷40 kPa) are osteogenic (Engler et al., 2006). Therefore, it is of great interest to functionalize scaffold surfaces with suitable coating materials whose mechanical properties could be fine tuned in order to vary substrate stiffness encompassing the physiological values of the specific tissue needed for the transplantation. Due to their many favorable and biomimetic properties, hydrogels have been increasingly recognized as promising biomaterials and have gained considerable attention in such biomedical engineering applications (Ibrahim et al., 2007; Ji et al., 2006; Takagi et al., 2006; Peppas et al., 2006). They can be chemically or physically modified under mild biocompatible conditions to exhibit specific cell–material interactions (Schante et al., 2011), furthermore, they can be designed to have elastic and loss moduli similar to those of soft tissue.

Among hydrogels, we focused on hyaluronic acid (HA), a well known linear polysaccharide composed of long chains of repeating disaccharide units of *N*-acetyl-D-glucosamine (GlcNAc) and D-glucuronic acid (GlcA) linked by β 1–4 glycosidic bond (Xu et al., 2012). Physiologically present in human body, its highest occurrence is in the extracellular matrix (ECM) of human connective tissue especially in the synovial fluid of joints, in the brain, in the dermis of the skin and in the vitreous body of the eye (Schante et al., 2011). Moreover, in physiological conditions HA is negatively charged and highly hydrophilic, surrounded by a sphere of water molecules linked by hydrogen bonds. Its strong hydrophilic character together with its high molecular weight values (10^5 Da in serum to 10^7 Da in the vitreous) (Burdick and Prestwich, 2011) give to HA both structural and functional roles in the body. Being a hydrogel based on naturally occurring carbohydrates, HA even offers the inherent advantages of being biocompatible and biodegradable by a complex enzymatic mechanism involving hyaluronidase enzymes (Gaffney et al., 2010). Finally, to improve its mechanical properties, to control the degradation rate and to prevent its rapid re-dissolution in water, HA can be chemically modified with crosslinking or conjunction reactions (Kenne et al., 2013; Bencherif et al., 2008; Yeom et al., 2010; Collins and Birkinshaw, 2007). Therefore HA is an appropriate biomaterial to reproduce mechanical substrate properties of native stem cells niches environment. To this end, numerous crosslinking methods have been reported and deeply studied to obtain biocompatible hydrogels including chemical and photochemical methods, the latter being much more suitable even for 3D cell encapsulation (Camci-Unal et al., 2013; Xiao et al., 2011). However, in the present work we aim to establish a simple, reliable and controlled methodology for the preparation and characterization of HA hydrogels encompassing the range of physiologically osteo-chondral relevant moduli to be used just as a scaffold coating material potentially mimicking the native ECM niches. With this aim, a homogeneous (Collins and Birkinshaw, 2011) crosslinking process was first optimized to obtain biocompatible chemical hydrogels using divinyl sulfone (DVS), highly reactive and efficient crosslinker, that creates ether linkages between HA primary hydroxyl groups, avoiding. Moreover, this is a single-step crosslinking method, no previous HA functionalization steps are needed (Schante et al., 2011; Ibrahim et al., 2010). Different HA crosslinking conditions process were tested in terms of crosslinking density (HA:DVS stoichiometric ratio) and crosslinking conditions (reaction time and temperature). Hydrogel mechanical properties were studied on macroscopic samples by dynamic rheological analysis with measurements of dynamic moduli and estimation of density of crosslinking; rheological results were successively benchmarked with swelling experiments following the Flory–Rehner theory (Flory, 1953), and by atomic force microscopy (AFM) nanoindentation which are experimental techniques much more suitable for the investigation of small-scale hydrogel samples as typically those coated onto scaffolds (Markert et al., 2013). The final goal is to keep a close control over the crosslinking process and to prepare HA hydrogels with tailored mechanical properties suitable as coating material for micrometric scaffold used to recreate osteo-chondral niches in vitro. It is also of great interest for our scope, the implementation and validation of characterization techniques, such as AFM nanoindentation experiments, that give the possibility to directly evaluate the mechanical properties of functionalized scaffolds without altering the sample.

2. Experimental section

2.1. Materials

Hyaluronic acid sodium salt (MW 1.6×10^6 g mol^{-1}) obtained by fermentation of *Streptococcus equi* bacteria—bacterial glycosaminoglycan polysaccharide; divinyl sulfone (DVS), sodium hydroxide (NaOH) and 1H,1H,2H,2H perfluorodecyltriethoxysilane (PFDTES, 97%) were all purchased from Sigma-Aldrich. All the reagents were used without any purification.

2.2. Hyaluronic acid hydrogels preparation

Hyaluronic acid hydrogels were prepared and chemically crosslinked using a homogeneous method based on previously described protocols (Collins and Birkinshaw, 2011), and involving addition of the crosslinking agent directly into the HA solution. Briefly, powdered HA was dissolved in alkaline solution (3% w/v, 0.2 M NaOH, pH 13) and DVS was added dropwised with three different HA:DVS molar ratio (1:2; 1:5 and 1:10 with respect to HA primary hydroxyls). The mixture was poured in a 50-mm Petri dish, after stirring it for 4 min in a closed vial to allow DVS uniform diffusion without its uncontrolled evaporation. The reaction was allowed to proceed at 4 °C and the gels were crosslinked at reaction different times (2 h; 12 h and 96 h). Both DVS-content and reaction time were varied in order to study the impact of these parameters on hydrogels mechanical properties. Each sample, representative of one crosslinking parameters combination, was prepared thrice. At the end of the curing processes, the gels were poured in excess water and washed several times in phosphate-buffered saline (PBS) to end the crosslinking reaction and to remove the potentially citotoxic unreacted DVS. The hydrogels were finally swollen at their equilibrium value for three days in a large excess of distilled water.

2.3. Rheological measurements

Storage (G') and loss (G'') moduli of hydrogels were measured using a Rheometrics Dynamic Stress Rheometer 200 operating under a 25 mm parallel-plate configuration and a 1.5 mm plate spacing. After preliminary stress sweep experiments to identify the linear viscoelastic range of the hydrogels, isothermal frequency sweep tests were performed considering a frequency range from 0.01 Hz to 1 Hz. The rubber elasticity theory was exploited to estimate both the Young's modulus E, assuming a Poisson's ratio of 0.5 (Hachet et al., 2012), and the crosslink density υ_{RH} of the hydrogel networks according to the following relationships

$$E = 2G'(1+\upsilon) \tag{2.1}$$

$$\upsilon_{RH} = \frac{G'}{RT} \tag{2.2}$$

where G' is the plateau storage modulus, R is the gas constant (8.314 J mol^{-1} K^{-1}) and T is the temperature at which the modulus was measured (310.15 K).

2.4. Thermogravimetric analysis, swelling measurements and Flory–Rehner calculations

Swelling experiments were conducted to measure the degree of mass swelling q_M of HA hydrogels which is strictly correlated to the mechanical strength of crosslinked networks and to their density of crosslinking (Anseth et al., 1996). Particularly, q_M was calculated as W_s/W_d which are respectively the weight of the equilibrium-swollen gel sample (W_s) and of the dried sample (W_d), and both were measured using a Q500 (TA Instrument) thermogravimetric analyzer (TGA). A small swollen piece of HA hydrogel, corresponding to W_s (40÷50 mg), was placed in the TGA weighing pan and slowly heated at 50 °C fixed-temperature until a constant mass, corresponding to W_d, was achieved. The crosslink density $\upsilon_{FR} = \rho_p/M_c$ was then assessed by applying an approximate expression of the Flory–Rehner equation valid for networks with low degrees of cross-linking swollen in good solvent (see Supporting information)

$$q_e^{5/3} \cong \frac{M_c}{\rho_p V_1}\left(\frac{1}{2}-\chi\right) \tag{2.3}$$

where M_c is the average molecular weight between crosslinks, V_1 is the molar volume of the solvent (18 cm^3 mol^{-1} for water), ρ_p is the density of the dry polymer (1.229 g cm^{-3}) χ is the Flory polymer–solvent interaction parameter (estimated to be 0.473 for HA in water based on several assumptions) (Baier Leach et al., 2003), and q_e is the volumetric swelling ratio determined from q_M (Marsano et al., 2000).

$$q_e = 1 + \frac{\rho_p}{\rho_s}(q_M - 1) \tag{2.4}$$

with ρ_s is the density of water.

2.5. AFM nanoindentation

AFM nanoindentation experiments in air were performed for a highly spatially resolved mechanical testing of the equilibrium-swollen HA hydrogels (Butt et al., 2005). Force-distance curves were obtained with an NSCRIPTOR™ atomic force microscope (Nanoink) in a controlled atmosphere chamber (T=+23 °C). The relative humidity was kept constant at 50% to minimize hydrogel water loss which can significantly influence their mechanical behavior (Anseth et al., 1996). A colloidal probe (series HYDRA6R-200NG-COLL, AppNano) with a nominal spring constant k_c=0.035 N m^{-1} and a spherical tip, made of SiO_2, was used in all measurements after its vapor phase silanization treatment with PFDTES (100 °C for 16 h in a sealed vial) to make the tip hydrophobic and to reduce the tip–gel adhesion phenomenon. All the nanoindentation curves were dynamically acquired with an indentation rate of 0.05 Hz. The maximum force applied onto the hydrogel surface in the elastic indentation range was 14.7±3.1 nN. In order to convert the cantilever deflection signal from mV (force-displacement) to nm (force-indentation), the deflection sensitivity of the instrument and so the sensitivity of the probe, was calculated from calibration measurements on a well cleaned Si wafer, assumed to be an infinitely rigid substrate (zero indentation). At least 20 nanoindentation curves were collected for each sample and results were averaged. The elastic modulus E was determined by fitting the Johnson–Kendall–Roberts (JKR) mathematical model with experimental data together with the geometrical features of the calibrated tip (Johnson et al., 1971). The JKR model, derived from the classical Hertzian relation (Sneddon, 1965), is suitable for spherical tips and soft sample with large adhesion force (Butt et al., 2005), and is represented by the following equations:

$$\delta = \frac{a^2}{R} - \frac{4}{3}\sqrt{\frac{aF_{ad}}{RE_{tot}}} \tag{2.5}$$

$$a = \left[\frac{R}{E_{tot}}\left(\sqrt{F_{ad}} + \sqrt{F + F_{ad}}\right)^2\right]^{1/3} \tag{2.6}$$

where δ the elastic indentation of the sample, a the contact radius, R is the tip radius (2.5÷4.5 μm), F_{ad} the pull-off force between the tip and the hydrogel surface, F the applied force and E_{tot} the reduced modulus.

Considering E_s, υ_s and E_t, υ_t the Young's moduli and the Poisson's ratios for the sample and the tip, respectively, the reduced modulus is defined as

$$\frac{1}{E_{tot}} = \frac{3}{4}\left(\frac{(1-\upsilon_s^2)}{E_s} + \frac{(1-\upsilon_t^2)}{E_t}\right) \tag{2.7}$$

Then, assuming the tip infinitely stiff and neglecting its deformation, Eq. (2.7) simplified to

$$\frac{1}{E_{tot}} = \frac{3}{4}\left(\frac{(1-\upsilon_s^2)}{E_s}\right) \tag{2.8}$$

The Young's modulus of the sample can also be expressed by the following equation using the JKR model

$$E_S = \frac{9}{4}(1-\nu_s^2)RF_{ad}\sqrt{\left(\frac{\left(3\sqrt{\frac{\Delta d}{\Delta d_{ad}}+1}-1\right)\left(\frac{1}{9}\left(\left(\sqrt{\frac{\Delta d}{\Delta d_{ad}}+1}\right)+1\right)\right)^{\frac{1}{3}}}{3R\delta}\right)^3} \tag{2.9}$$

where Δd is the range of cantilever deflection considered in the contact part of the force curve for calculating the modulus and Δd_{ad} the pull-off cantilever deflection in the withdrawn curve.

For all measurements υ_s was assumed to be 0.5 (Flores-Merino et al., 2010). According to the JKR theory, the location

of the point of zero indentation is established from the force curve where the applied force $F = -(8/9)\ F_{ad}$, as obtained by setting $\delta = 0$ in Eq. (2.5), substituting the definition of contact radius given by Eq. (2.6) and solving for F (Lin et al., 2007).

Young moduli E_{AFM} obtained with nanoindentation were compared with E_{RH} values derived from rheological measurements taking into account that the two analyses were performed at different temperature, parameter affecting the mechanical behavior of rubbery materials. E_{RH} (23 °C) was therefore calculated fitting Eq. (2.1) with $G' = \upsilon_{RH} RT$ where $T = 296.15$ K and υ_{RH} previously estimated with Eq. (2.2).

3. Results and discussion

3.1. Hydrogels preparation

Hyaluronic acid hydrogels were prepared from HA aqueous solution (3% w/v) crosslinking with divinyl sulfone. In order to avoid DVS evaporation and irreproducibility of results due to not homogenously crosslinked hydrogels, the reaction was allowed to proceed at low temperature (≈ +4 °C) in closed vials. A total of nine hydrogels were prepared varying crosslinking agent content and curing time (Tables 1 and 2).

Table 1 – AFM tip dimensions and indentation depth.

Tip radius R [μm]	Indentation depth δ [nm]
2.5 ÷ 4.5	230 ÷ 800

Table 2 – Summary of hydrogels samples prepared with HA:DVS stoichiometric ratios (column 2) and reaction times investigated (column 3).

Sample [h]	HA:DVS	t_{ret} [h]
HA3%_1/2_2	1:2	2
HA3%_1/2_12	1:2	12
HA3%_1/2_96	1:2	96
HA3%_1/5_2	1:5	2
HA3%_1/5_12	1:5	12
HA3%_1/5_96	1:5	96
HA3%_1/10_2	1:10	2
HA3%_1/10_12	1:10	12
HA3%_1/10_96	1:10	96

3.2. HA:DVS hydrogels characterization

A reliable methodology based on three independent techniques was used to test the mechanical behavior of DVS-crosslinked swollen hydrogels: rheological analysis, swelling ratio measurements with Flory–Rehner calculations, and AFM nanoindentation. While rheology is a consolidated method giving the most reliable experimental results that allows to directly evaluate the crosslinking efficiency, it is unsuitable to test small size samples as those typically used for coating scaffolds. In those conditions thermogravimetric experiments and/or AFM measurements can be alternatively carried out. However, their reliability has to be assessed with proper cross-check experiments.

3.2.1. Rheology

Rheological measurements were carried out for swollen gels after three days of immersion in deionized water. The viscoelastic behavior of 3% HA solution without DVS was also considered. According to the experimental curves obtained (data not shown in the graph) HA solution behaves as a viscous liquid with $G'' > G'$ in all frequency range explored. After covalent crosslinking HA molecules (Figs. 1–3), the elastic component prevails with storage modulus almost independently on frequency and always higher than loss modulus for all HA3%_1/10 samples. Similar behavior but with lower G' plateau values are shown by HA3%_1/5 samples.

For the sample HA3%_1/2_2 h a sol–gel transition at 0.1 Hz is observed suggesting incomplete crosslinking. A qualitatively similar behavior was observed also for the others HA3%_1/2 samples although with much lower crossover frequency (higher molecular weight). We assumed HA3%_1/2_2 h parameters conditions (2 h curing time, HA:DVS = 1:2) as threshold

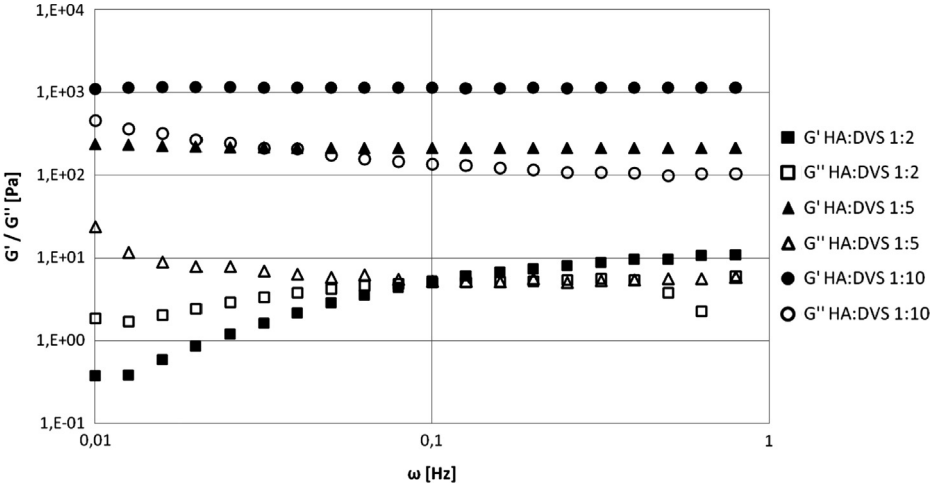

Fig. 1 – Viscous (G'') and elastic (G') modulus components for hydrogels obtained after 2 h of curing. While the HA3%_1/10 and HA3%_1/5 behave as crosslinked hydrogels with G' predominating over G'', the HA3%_1/2 has a change from viscous liquid behavior ($G'' > G'$) at lower frequencies to elastic solid behavior ($G'' < G'$) at higher frequencies.

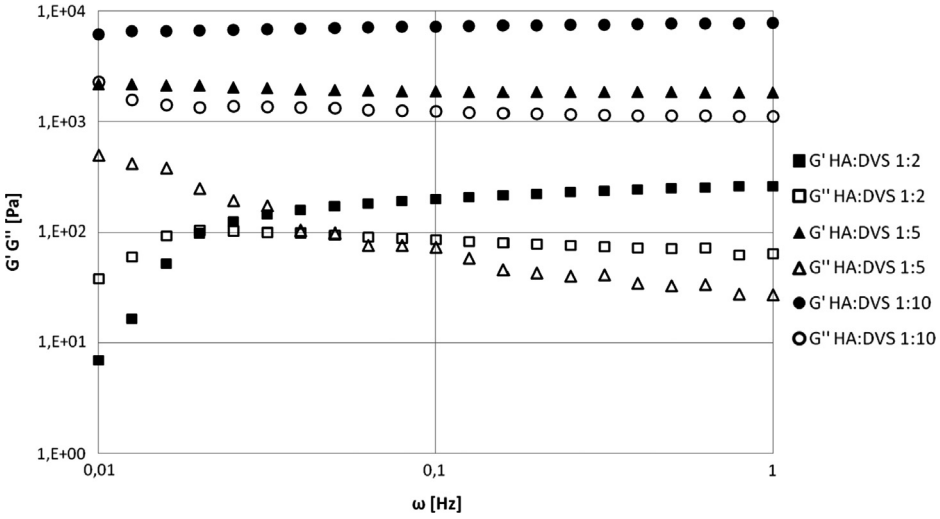

Fig. 2 – Viscous (G'') and elastic (G') modulus components for hydrogels obtained after 12 h of curing. Increasing in crosslinking reaction time till 12 h, without changing in DVS content, lead to elastic and viscous moduli enhancement. A crossover phenomenon is still observed for HA3%_1/2.

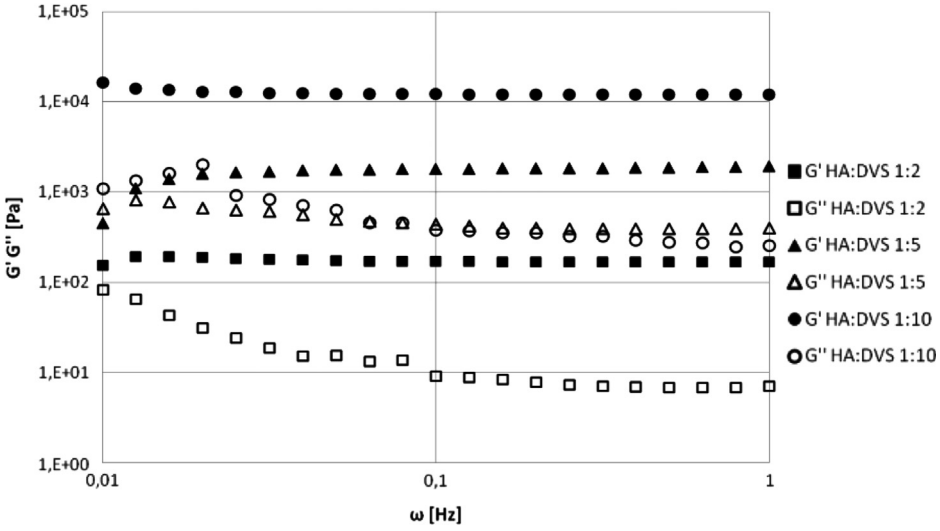

Fig. 3 – Viscous (G'') and elastic (G') modulus components for hydrogels obtained after 96 h of curing. Elastic and viscous moduli are almost constant within all frequency range, with G' predominating over G''. Further moduli enhancement, even if restrained, is observed comparing to 12 h of curing moduli values.

values to efficiently crosslink HA. Results showed that both stoichiometric ratio and reaction times can be used to fine tune the hydrogel stiffness to the desired value. Actually, according to Eq. (2.1) the corresponding Young's moduli E_{RH} are in the range from 0.03 kPa to 37 kPa (Table 3).

Extending the reaction time without varying DVS content is efficient to strengthen hydrogels; increasing from 2 h to 12 h led to an enhancement in G' of nearly an order of magnitude, whereas extending curing time till 96 h has a minor effect. This may allow for a reduction of DVS quantities with better hydrogel biocompatibility or less laborious washing treatments.

Finally, the cross-linking density υ_{RH} of the networks was estimated according to Eq. (2.2), and results are shown in Table 3 (column 6). Actually υ_{RH} values range from 4.18E-09 mol cm^{-3} to 4.08E-06 mol cm^{-3}.

3.2.2. *Swelling ratio determinations and Flory–Rehner calculations*

The extent of swelling of hydrogels can be related to their density of crosslinking. The swelling was measured through thermogravimetric analysis, using the Flory–Rehner theory to calculate both the molecular weights between cross-links M_c and crosslink densities υ_{FR}. As data reported in Table 3 showed, as DVS content and curing time increased, swelling ratio q_M decreased, indicating higher levels of crosslinking which is in accordance with the theory of rubber elasticity (Treloar, 2005).

Flory–Rehner calculations showed that increased HA:DVS stoichiometric ratio and curing time led to decreased molecular weights between cross-links (ranging from 86.2E+06 g mol^{-1} for HA:DVS 1/2 curing time 2 h, to 3.06E+05 for HA:DVS

Table 3 – Comparison of numerical values obtained from rheological experiments (RH) and TGA analysis (FR). Storage modulus G' and crosslink density υ are reported for both methods, whereas for TGA even swelling ratio q_M and molecular weight between cross-links M_c are presented. G' and υ TGA values resulted in good agreement with rheological ones attesting the trend of hydrogels enhancing with increasing both curing time and DVS content.

Sample [h]	G'_{RH} [kPa]	υ_{RH} [mol cm^{-3}]	q_M	M_c [g mol^{-1}]	υ_{FR} [mol cm^{-3}]	G'_{FR} [kPa]
HA3%_1/2_2	0.01±0.003	4.18E-09±1.2E-09	839.56	86.2E+06	1.42E-08±2.6E-09	0.037±0.007
HA3%_1/2_12	0.17±0.01	6.47E-08±5.6E-09	781.88	76.6E+06	1.60E-08±4E-09	0.041±0.01
HA3%_1/2_96	0.19±0.01	6.77E-08±5.6E-09	552.46	42.9E+06	3.28E-08±6E-09	0.084±1.5E-02
HA3%_1/5_2	0.21±0.01	8.45E-08±5.6E-09	331.46	18.3E+06	9.63E-08±1.2E-08	0.25±3.1E-02
HA3%_1/5_12	1.5±0.5	5.95E-07±1.8E-07	120.12	4.47E+06	4.93E-07±2.27E-07	1.27±5.8E-01
HA3%_1/5_96	1.87±0.41	7.26E-07±1.6E-07	79.03	1.6E+06	8.32E-07±1.4E-07	2.14±3.5E-01
HA3%_1/10_2	1.11±0.04	4.43E-07±1.65E-08	161.67	5.53E+06	4.93E-07±3.3E-07	1.27±8.6E-01
HA3%_1/10_12	7.5±2.2	2.92E-06±8.5E-07	50.95	8.03E+05	1.19E-06±4.8E-07	3.06±1.2
HA3%_1/10_96	12.4±0.9	4.08E-06±3.5E-07	28.63	3.06E+05	5.37E-06±1.9E-06	1.39E+01±4.9

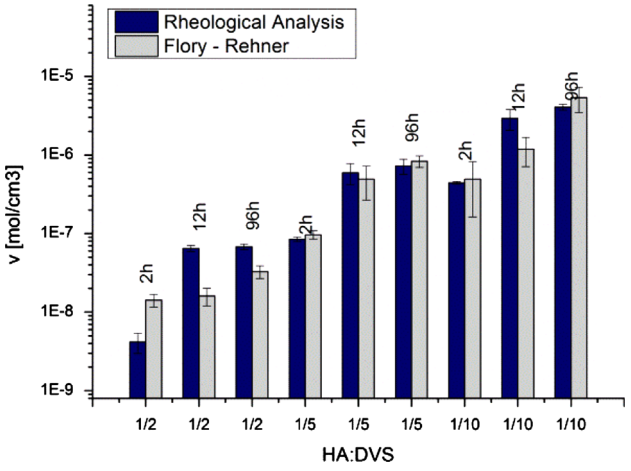

Fig. 4 – Comparison of crosslink density υ values obtained with rheology and TGA analysis.

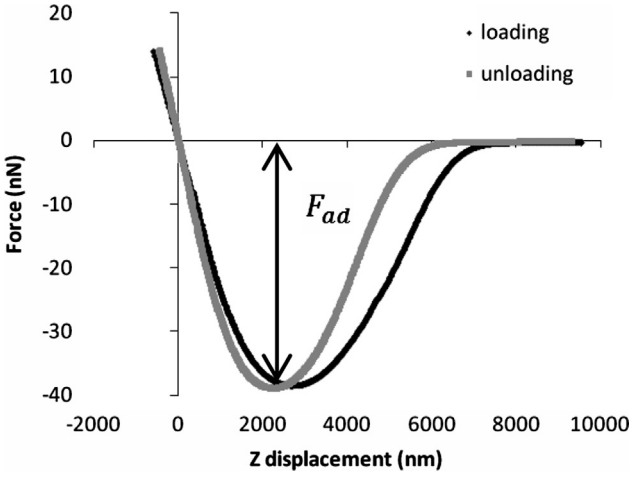

Fig. 5 – Force-distance curves of HA3%_1/5_12 h sample. The jump in the signal deflection affecting both the loading and the unloading curves is due to the strong tip-substrate adhesion phenomena as a consequence of the presence of an aqueous meniscus on the hydrogel sample. The hysteresis attested a viscoelastic dissipation.

1/10 curing time 96 h), as well as increased crosslink density υ_{FR} (ranging from 1.42E-08 mol cm^{-3} to 5.37E-06 mol cm^{-3}). Those data were used for fitting Eq. (2.2) in order to calculate G'_{FR}. The difference between G'_{RH} and G'_{FR} experimental values ranges from a minimum of 0.027 kPa to a maximum of 4.14 kPa, anyway the two sets of values are in good agreement (Fig. 4) although based on completely different approaches.

TGA could be implemented in future works as an easy and reliable way to indirectly evaluate the mechanical characteristic of scaffold thin coatings, just sampling a few milligrams of HA from the functionalized scaffold surfaces, necessary to be sensed in the TGA weighing pan.

3.2.3. *AFM nanoindentation*

Finally, Young's moduli E_{AFM} of 1:5 and 1:10 HA:DVS crosslinked samples were measured also from the force-distance curves obtained randomly indenting HA hydrogel surfaces. AFM nanoindentation of hydrogels is often carried out in liquid phase. The technique is not however applicable to any AFM instrument and its major drawback is the difficult laser setting on the cantilever, and the disturbed signal on the photodiode due to the refraction given by the water–air interface. On the other hand the main problem arising from AFM nanoindentation in air (as the technique adopted in this work) is the possibility of strong tip-substrate adhesion phenomena, typical of very flexible cantilevers. Actually several problems were met in our case while approaching the sample because the tip was suddenly attracted towards the sample making it difficult to identify the tip/gel surface contact point, and impossible to remove it during the unloading step. Tip-substrate adhesion was effectively minimized – although not completely eliminated – by carrying out a gas-phase hydrophobization of the tip (see Section 2). The residual adhesion can be taken into account using the JKR model instead of the classical Hertz equation. The jump in the signal deflection was observed both in the loading and unloading curves.

By comparing the experimental results (Figs. 5 and 6), it is noteworthy to observe that the HA3%_1/10_12 h sample showed a perfectly elastic behavior with loading and unloading curves totally overlapped. On the contrary the softer HA3%_1/5_12 h sample showed a hysteresis due to a higher viscoelastic dissipation induced by the lower degree of

crosslinking of the sample. Moreover, while approaching the tip deflection was anticipated for the latter sample. Probably, this is due to the difference in water content of the two samples, previously attested with q_M swelling measurements (Table 3), which leads to differences in adhesion force F_{ad}. This force was calculated according to the Hooke's law from the pull-off cantilever deflection as $F_{ad} = k_c \Delta d_{ad}$ (Table 4).

The mathematical JKR model (Eq. (2.9)), suitable for soft sample and taking into account the adhesive component, was used to estimate Young modulus E_{AFM} starting from experimental data and tip geometrical characteristics. E_{AFM} average values turned out to be about 32 kPa for HA3%_1/5 and 72 kPa for HA3%_1/10 (Table 4). They indicated increasingly stiffer hydrogels with increasing HA:DVS content confirming the trend seen with previous characterization. We also observed that Young's modulus measured by AFM varied depending on the selection of indentation depths: the variation of the indentation depth from 400 nm to 800 nm could result in a decrease of E_{AFM} from 47 kPa to 20 kPa for HA3%_1/5. Similarly, HA3%_1/10 showed a modulus of 79 kPa at small indentation depth of 230 nm and its behavior at larger indentation depths (350 nm) revealed a value of 54 kPa.

These E_{AFM} values were compared with E_{RH} values derived from rheological measurements (Ouasti et al., 2011) calculated exploiting Eqs. (2.1) and (2.2), taking into account that the two analyses were performed at different temperature (see Section 2) and the sources of uncertainty in AFM-based materials property measurements (Clifford and Seah, 2005; Lin and Horkay, 2008; Wagner et al., 2011). The values of elastic modulus obtained from AFM nanoindentation resulted rather higher than those from rheology, likely because AFM experiments were performed in air, leading the hydrogels to partially lose water during the measurement and to get slightly stiffer than those completely swollen in water (Table 4). This phenomenon mainly affected the HA3%_1/5 E_{AFM}–E_{RH} values due to its higher water content with respect to HA3%_1/10, in accordance with swelling ratios q_M (Table 3). Further investigations are needed to systematically minimize this gap, both estimating the actual hydrogel water content during the measurement with proper gravimetric analyses and understanding the effect of the selected indentation depth range on the estimation of the elastic modulus.

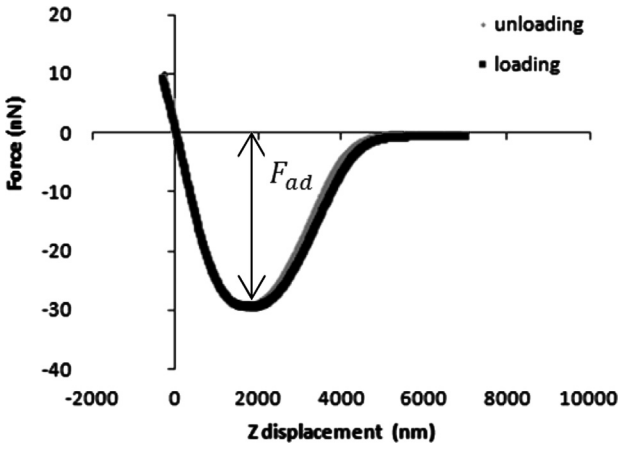

Fig. 6 – Force-distance curves of HA3%_1/10_12 h sample: the complete overlapping of the two curves in the linear phase of the signal, attested a perfect elastic behavior of the sample.

4. Conclusions

In the present work, we presented an in-depth study of the process for chemically crosslinking HA hydrogels allowing to fine tune their physical properties. Particularly, we meant to obtain hydrogels with mechanical properties closely approximating those of natural stem cells ECM niches. We first optimized the crosslinking procedure for HA/DVS hydrogels synthesis. Then, we aimed to understand the effect that varying DVS content and curing time have on HA hydrogels stiffness which was evaluated through rheology, swelling measurements and first AFM nanoindentation experiments. The first technique is a consolidated and well-known method giving the most reliable experimental results and it allows to directly evaluate the crosslinking efficiency through the Elastic and Viscous moduli measurements. However it can be performed over macroscopic sample and it results unsuitable for small-sized hydrogels samples. Rheological results were benchmarked and used to assess the viability of the others two techniques which are experimentally harder but much more suitable for mechanical properties investigation at the microscale. Particularly, for swelling experiments just few milligrams of hydrogels should be collected from the coated scaffold surfaces, whereas AFM nanoindentation could be directly implemented on the hydrogel grafted onto micrometric structures. The good agreement between rheological and thermogravimetric characterization data proved both the repeatability and reliability of samples preparation. Very interestingly, our results demonstrated that combining crosslinking parameters it was possible to prepare samples with Young's moduli in the range from 0.03 kPa to 37 kPa largely included in the stem cells niches physiological range. Moreover, it was possible to strengthen the materials just increasing curing time without varying DVS content, gaining in biocompatibility. This highlights that these hydrogels are suitable candidate as micrometric scaffold surfaces coating to be implemented in regenerative medicine for engineering stem-cells niches. Further improvements in AFM nanoindentation analyses, suggested to be the best small-sized sample

Table 4 – Numerical values for AFM nanoindentation experiments on HA3%_1/5_12 h and HA3%_1/10_12 h samples. The elastic indentation of the samples (δ), the adhesion force (F_{ad}) and the elastic modulus (E_{AFM}) are reported. In the last column the elastic moduli obtained from rheology (E_{RH}) are reported as comparison.

Sample [h]	δ [nm]	F_{ad} [nN]	E_{AFM} (JKR) [kPa]	E_{RH} (23 °C) [kPa]
HA3%_1/5_12	567.77 ± 65.68 (400 ÷ 800)	38.47 ± 0.31	32.40 ± 4.23 (20 ÷ 47)	4.4 ± 0.4
HA3%_1/10_12	281.57 ± 16.88 (230 ÷ 350)	29.45 ± 5.89	72.13 ± 3.24 (54 ÷ 79)	21.6 ± 6.3

characterization technique, will give the chance to directly evaluate HA-coated micrometric scaffold mechanical properties.

Appendix A. Supplementary material

Supplementary data associated with this article can be found in the online version

REFERENCES

Anseth, K.S., Bowman, C.N., Brannon-Peppas, L., 1996. Mechanical properties of hydrogels and their experimental determination. Biomaterials 17 (17), 1647–1657.

Baier Leach, J., et al., 2003. Photocrosslinked hyaluronic acid hydrogels: natural, biodegradable tissue engineering scaffolds. Biotechnol. Bioeng. 82 (5), 578–589.

Bencherif, S.A., et al., 2008. Influence of the degree of methacrylation on hyaluronic acid hydrogels properties. Biomaterials 29 (12), 1739–1749.

Burdick, J.A., Prestwich, G.D., 2011. Hyaluronic acid hydrogels for biomedical applications. Adv. Mater. 23 (12), H41–H56.

Butt, H.-J., Cappella, B., Kappl, M., 2005. Force measurements with the atomic force microscope: technique, interpretation and applications. Surf. Sci. Rep. 59 (1–6), 1–152.

Camci-Unal, G., et al., 2013. Synthesis and characterization of hybrid hyaluronic acid-gelatin hydrogels. Biomacromolecules 14 (4), 1085–1092.

Clifford, C.A., Seah, M.P., 2005. Quantification issues in the identification of nanoscale regions of homopolymers using modulus measurement via AFM nanoindentation. Appl. Surf. Sci. 252 (5), 1915–1933.

Collins, M.N., Birkinshaw, C., 2007. Comparison of the effectiveness of four different crosslinking agents with hyaluronic acid hydrogel films for tissue-culture applications. J. Appl. Polym. Sci. 104 (5), 3183–3191.

Collins, M.N., Birkinshaw, C., 2011. Morphology of crosslinked hyaluronic acid porous hydrogels. J. Appl. Polym. Sci. 120 (2), 1040–1049.

Discher, D.E., Janmey, P., Wang, Y.-l., 2005. Tissue cells feel and respond to the stiffness of their substrate. Science 310 (5751), 1139–1143.

Engler, A.J., et al., 2006. Matrix elasticity directs stem cell lineage specification. Cell 126 (4), 677–689.

Evans, N.D., et al., 2009. Substrate stiffnessaffects early differentiation events in embryonic stem cells. Eur. Cells Mater., 1–1418, 1–14.

Flores-Merino, M.V., et al., 2010. Nanoscopic mechanical anisotropy in hydrogel surfaces. Soft Matter 6 (18), 4466–4470.

Flory, P.J., 1953. Principles of Polymer Chemistry. xvi. Cornell University Press, Ithaca; London672.

Gaffney, J., et al., 2010. Therapeutic applications of hyaluronan. Molecular Biosystems 6 (3), 437–443.

Hachet, E., et al., 2012. Design of biomimetic cell-interactive substrates using hyaluronic acid hydrogels with tunable mechanical properties. Biomacromolecules 13 (6), 1818–1827.

Ibrahim, S., Kang, Q.K., Ramamurthi, A., 2010. The impact of hyaluronic acid oligomer content on physical, mechanical, and biologic properties of divinyl sulfone-crosslinked hyaluronic acid hydrogels. J. Biomed. Mater. Res. Part A 94A (2), 355–370.

Ibrahim, S., et al., 2007. A surface-tethered model to assess size-specific effects of hyaluronan (HA) on endothelial cells. Biomaterials 28 (5), 825–835.

Ji, Y., et al., 2006. Electrospun three-dimensional hyaluronic acid nanofibrous scaffolds. Biomaterials 27 (20), 3782–3792.

Johnson, K.L., Kendall, K., Roberts, A.D., 1971. Surface energy and the contact of elastic solids. Proc. R. Soc. London Ser. A. Math. Phys. Sci. 324 (1558), 301–313.

Kenne, L., et al., 2013. Modification and cross-linking parameters in hyaluronic acid hydrogels—definitions and analytical methods. Carbohyd. Polym. 91 (1), 410–418.

Kim, I.L., Mauck, R.L., Burdick, J.A., 2011. Hydrogel design for cartilage tissue engineering: a case study with hyaluronic acid. Biomaterials 32 (34), 8771–8782.

Lin, D.C., Dimitriadis, E.K., Horkay, F., 2007. Robust strategies for automated AFM force curve analysis—II: Adhesion-influenced indentation of soft, elastic materials. J. Biomech. Eng. 129 (6), 904–912.

Lin, D.C., Horkay, F., 2008. Nanomechanics of polymer gels and biological tissues: a critical review of analytical approaches in the Hertzian regime and beyond. Soft Matter 4 (4), 669–682.

Markert, C.D., et al., Characterizing the micro-scale elastic modulus of hydrogels for use in regenerative medicine. Journal of the Mechanical Behavior of Biomedical Materials, (0).

Marsano, E., et al., 2000. Behaviour of gels based on (hydroxypropyl) cellulose methacrylate. Polymer 41 (21), 7691–7698.

Ouasti, S., et al., 2011. Network connectivity, mechanical properties and cell adhesion for hyaluronic acid/PEG hydrogels. Biomaterials 32 (27), 6456–6470.

Peppas, N.A., et al., 2006. Hydrogels in biology and medicine: from molecular principles to bionanotechnology. Adv. Mater. 18 (11), 1345–1360.

Schante, C.E., et al., 2011. Chemical modifications of hyaluronic acid for the synthesis of derivatives for a broad range of biomedical applications. Carbohyd. Polym. 85 (3), 469–489.

Sneddon, I.N., 1965. The relation between load and penetration in the axisymmetric boussinesq problem for a punch of arbitrary profile. Int. J. Eng. Sci. 3 (1), 47–57.

Takagi, A., et al., 2006. Incorporation into a biodegradable hyaluronic acid matrix enhances *in vivo* efficacy of recombinant human interleukin 11 (rhIL11). J. Controlled Release 115 (2), 134–139.

Treloar, L.R.G., 2005. The Physics of Rubber Elasticity, third ed.xii. Clarendon Press, Oxford310.

Wagner, R., et al., 2011. Uncertainty quantification in nanomechanical measurements using the atomic force microscope. Nanotechnology 22 (45), 455703.

Xu, X., et al., 2012. Hyaluronic acid-based hydrogels: from a natural polysaccharide to complex networks. Soft Matter 8 (12), 3280–3294.

Yeom, J., et al., 2010. Effect of cross-linking reagents for hyaluronic acid hydrogel dermal fillers on tissue augmentation and regeneration. Bioconjugate Chem. 21 (2), 240–247.